Materials Science and Engineering A 527 (2010) 7770–7774

Contents lists available at ScienceDirect

Materials Science and Engineering A

journal homepage: www.elsevier.com/locate/msea

Precipitation and clustering in the early stages of ageing in Inconel 718

Talukder Alam[a,*], Mahesh Chaturvedi[b], Simon P. Ringer[a], Julie M. Cairney[a]

[a] Australian Centre for Microscopy and Microanalysis, The University of Sydney, NSW 2006, Australia
[b] Department of Mechanical and Industrial Engineering, The University of Manitoba, Winnipeg, MB R3T 5V6, Canada

ARTICLE INFO

Article history:
Received 12 February 2010
Received in revised form 17 August 2010
Accepted 18 August 2010

Keywords:
Atom probe FIM
Electron microscopy
Nickel based superalloys
Age hardening
Ageing
Precipitation

ABSTRACT

In this report we investigate the onset and evolution of precipitation in the early stages of ageing in the alloy WE 91, a variant of the Ni–Fe–Cr superalloy Inconel 718 (IN718). Transmission electron microscopy and atom probe tomography were used to study the size and volume fraction of γ′ and γ″ precipitates and the extent of pre-precipitate clustering of Al/Ti and Nb.

Co-located γ′ and γ″ precipitates were observed from the shortest ageing times that precipitates could be visualised using atom probe. At shorter times, prior to the observation of precipitates, clustering of Al/Ti and Nb was shown to occur. The respective volume fraction of the γ′ and γ″ precipitates and the clustering of Al/Ti and Nb suggest that γ″ nucleates prior to γ′ during ageing at 706 °C for this alloy.

1. Introduction

Extreme environments in jet engines and power generators require the excellent mechanical and chemical properties at high temperature and high stress displayed by superalloys. Good creep properties, corrosion resistance and wear resistance at operating temperatures are of paramount importance. The Ni-based superalloy Inconel 718 (IN718), which has an operating range of 600–650 °C, combines all these attributes with the added advantage of good weldability [1]. Because of the high cost involved in the production of superalloys and replacement of engines, welding is used to repair damage during routine service. Thus IN718 has found widespread usage in components like blades and disks in gas turbine engines and steam turbines [2–4].

The two precipitates that contribute to the hardness of IN718 are the $L1_2$ ordered γ′ phase (Ni_3Al or Ni_3Ti), and the DO_{22} ordered γ″ phase (Ni_3Nb) [1–7]. Good weldability in this alloy is generally attributed to the sluggishness of the γ″ age-hardening reaction, which allows relief of residual weld stresses during heat treatment prior to the nucleation and growth of the γ″ precipitates [7]. Many years of extensive study by various researchers has led to an understanding of the morphology and distribution of these precipitates once established. However, less is known about the onset of formation of these phases in the early stages of ageing. In this report we shed light on the very early stages of nucleation and precipitation in IN718, relating the hardness to the microstructure at short ageing times.

Previous studies of nucleation and precipitation of γ′ and γ″ in Ni-based superalloys have predominantly utilised TEM dark field techniques to image these phases. However, for very short ageing times the precipitates are exceedingly small and it is extremely difficult to resolve the particles using dark field imaging on even the best transmission electron microscopes. Slama et al. [8,9] studied the age hardening and the microstructure of IN718 at various temperatures by X-ray diffraction and TEM at relatively long ageing times, with the smallest time being an hour. Nakai et al. [10] reported results of ageing of IN718 for relatively short periods, comparing ageing time and solution treatments. These latter investigators focused on the interaction of the γ′ and γ″ precipitates with dislocation dipoles using transmission electron microscopy (TEM), but less on the nucleation sequence.

Atom probe tomography can provide 3D atomic-scale maps of atoms with resolution close to 0.1 nm in both the depth and lateral direction. Miller [11], and Burke and Miller [12,13] have previously undertaken a number of studies of precipitation in Inconel 718 after multiple stage heat treatments. They have confirmed the formation of lenticular γ″ precipitates after 8 h of ageing at 870 °C, providing details of concentration enrichments and depletions near the γ″ precipitate–γ matrix interface. Further ageing at 600 °C or 760 °C resulted in the formation of much smaller, secondary precipitates consisting of layers of γ′ and γ″. Similar 'secondary' γ″ precipitates were observed in specimens aged at 760 °C for 8 h without

* Corresponding author at: The Australian Centre for Microscopy and Microanalysis, The University of Sydney, NSW 2006, Australia. Tel.: +61 2 9351 7679; fax: +61 2 9351 7682.
E-mail address: talukder.alam@sydney.edu.au (T. Alam).

0921-5093/$ – see front matter © 2010 Elsevier B.V. All rights reserved.
doi:10.1016/j.msea.2010.08.053

Table 1
Nominal composition of WE 91.

	Elements											
	C	Mo	Cr	Fe	Nb	Ti	Al	Ni	Mg	S[a]	P[a]	B[a]
at.%	0.029	1.751	19.878	18.841	3.416	1.214	1.163	53.706	14	6	220	110

[a] Value in ppm.

the 870 °C intermediary step; however, the composition of these precipitates was closer to that of the primary γ″ phase.

This study utilises both TEM and atom probe tomography (APT) to investigate ageing in IN718, comparing Vickers microhardness data to the microstructural information. Data mining techniques were applied to the atom probe datasets to detect pre-precipitation clustering of the constituent elements that can provide information about the precipitation sequence in this alloy.

2. Experimental details

The sample investigated in this study is known as WE 91. This alloy is a variant of IN718 with trace additions of B and P that have been included to improve the creep performance. The composition is shown in Table 1. The sample was solution treated at 1050 °C for 45 min and oil quenched. Ageing was then carried out at 706 °C in a tube furnace in air and the sample quenched in water. Vickers microhardness testing was carried out after each stage of heat treatment using a LECO hardness tester with a load of 0.3 kg and a 10 s dwell time. The same specimen was then aged further for subsequent examination (i.e. the ageing time was cumulative).

TEM and atom probe specimens were prepared using standard electropolishing techniques [14,15]. TEM work was undertaken on a Philips CM12. Atom probe data was collected using an Imago LEAP3000XSi operating in voltage mode at a pulsing frequency of 200 kHz. The evaporation rate was kept constant at 0.5% and a pulse fraction (PF) of 25% was used.

There are a number of parameters on the atom probe that either directly or indirectly affect the quality of the acquired data [14]. To ensure that the data was of the highest quality and suitable for clustering calculations, a series of experiments were firstly conducted with varied operating parameters to find the most suitable running conditions. With the objective of attaining the highest signal-to-noise ratio and mass resolution, the optimum temperature and flight path length during the acquisition were determined for a given evaporation rate and pulse fraction. After these detailed test-runs to determine the optimum parameters for data collection the temperature and flight length were set at 40 K and 125 mm, respectively.

Reconstruction and visualisation of the atom probe data was performed using the commercial software IVAS© (Imago Scientific). Clustering analysis was carried out using the 'Core Linkage' algorithm developed by Stephenson et al. [16].

3. Results and discussion

As shown in Fig. 1, the hardness of IN718 after 41,400 s (11.5 h) of ageing at 706 °C is about 2.5 times that of the as-quenched (AQ) state. The overall trend shows that the hardness increases as a function of ageing time and does not appear to have peaked yet. This is consistent with the observations of Nakai et al. [10], who undertook similar ageing experiments. Although the ageing in the work by Slama et al. [8,9] was mostly undertaken for much longer ageing times, their data from a specimen aged at 720 °C is also broadly in agreement with the current results (ageing for longer periods revealed a hardness peak at 50 h). Samples at four ageing times were chosen for APT and TEM examination. These are marked A, B, C and D, respectively, in Fig. 1. The first sample is in the AQ state. The second sample, after 120 s of ageing, was selected as it represents the first signs of an increase in hardness. The third and fourth samples have been aged for 500 s and 5000 s, respectively, after which significant hardening has been observed to occur.

Imaging and selected area diffraction TEM studies were used to investigate the formation of γ′ and γ″ precipitates (Figs. 2 and 3). Indexed selected area diffraction patterns from the [0 0 1] zone axis for specimens aged for 120 s and 5000 s are shown in Figs. 2b and 3b, respectively. The ⟨0 0 1⟩ and ⟨0 1 1⟩ type superlattice reflections can arise from both the $L1_2$-ordered γ′ and the DO_{22}-ordered γ″ precipitates, while the ⟨½ 1 0⟩ reflections can only be associated with the γ″ phase [17,18]. The specimen aged for 120 s showed no evidence of precipitation in the form of superlattice reflections (Fig. 2b), whereas the specimen aged for 5000 s showed clear evidence of γ″ (Fig. 3b). The specimen aged for 500 s (not shown) showed the same superlattice reflections, but of lower intensity, as the one aged for 5000 s. Some mottled contrast was observed in the bright field image from the specimen aged for 5000 s (Fig. 3a). However, due to the difficulty of obtaining clear dark field images from such small precipitates (they are thought to be just a few nm in size), no information is available about the morphology or the relative distribution of γ″ and γ′ if present.

Atom probe datasets from the specimens aged for 120 s, 500 s and 5000 s are shown in Fig. 4a–c, respectively. Isoconcentration surfaces (10 at.%) of Al + Ti (in the images on the left) and Nb (in the images on the right) are used to reveal the presence and of both γ′ and γ″ precipitates along with their distribution, size and location.

Consistent with the TEM results, atom probe investigations did not reveal any evidence of precipitation in the specimen that had undergone 120 s of ageing at 706 °C (Fig. 4a). However, after 500 s of ageing, small γ′ and γ″ precipitates can be observed in the atom probe data (Fig. 4b). At this stage the γ′ precipitates are 2–3 nm in size and the γ″ precipitates are 2–5 nm. Both types of precipitates increase in size with additional heat treatment; after 5000 s of ageing γ′ and γ″ are 5–15 nm and 10–15 nm in size, respectively. The γ′ and γ″ precipitates are located in the same regions, indicating that

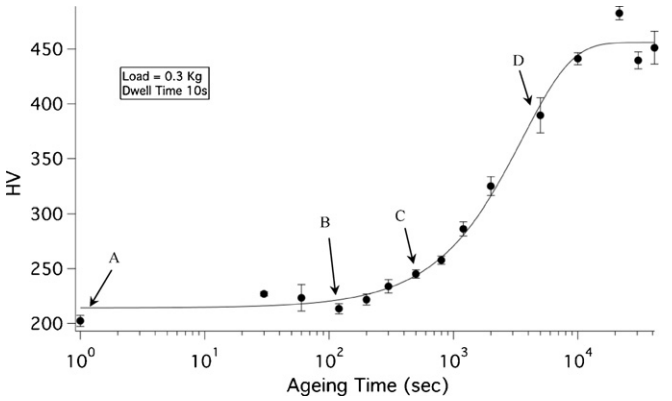

Fig. 1. The plot of Vicker's hardness with ageing time at 706 °C. Samples at positions A–D on the curve were selected for subsequent examination using TEM and APT. The error bars shown are the standard deviation of 10 hardness measurements and the line between data points is included to guide the eye only.

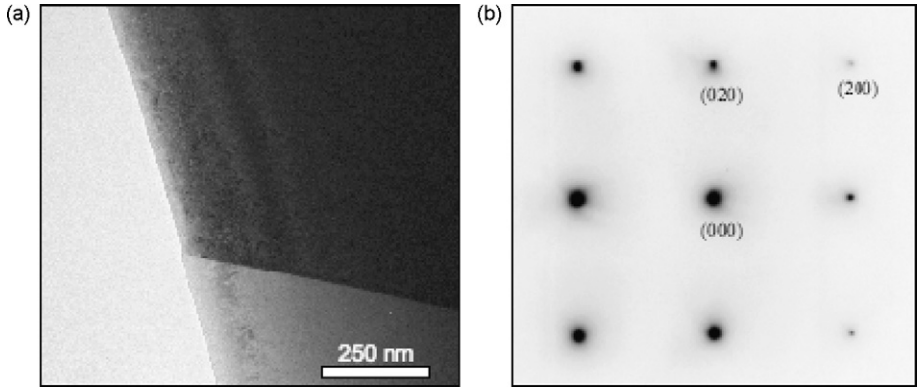

Fig. 2. TEM images of the sample aged for 120 s. a) Bright field image. b) Diffraction pattern taken from the [0 0 1] zone axis. The absence of extra reflections indicates that no precipitation can be discerned using this technique at this stage of ageing.

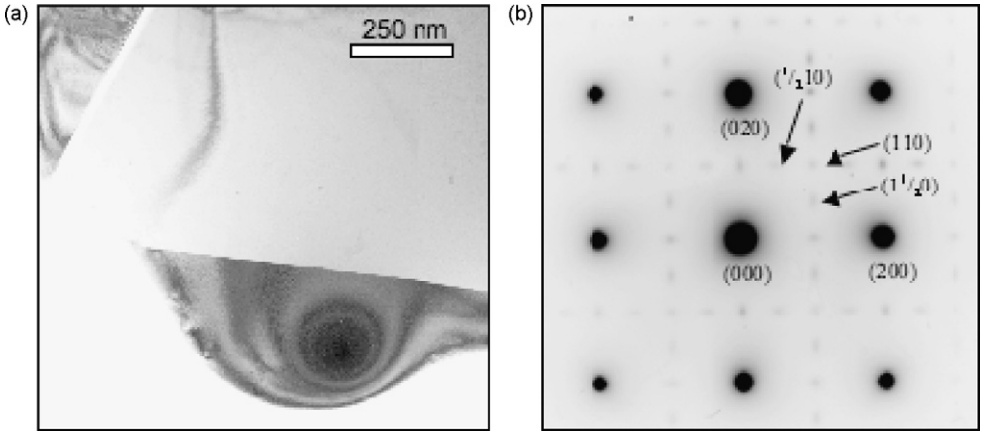

Fig. 3. TEM images of the sample aged for 5000 s. a) Bright field image. b) Diffraction pattern taken from the [0 0 1] zone axis. Extra reflections confirm the presence of γ′ and γ″ precipitates.

they are very often in the form of co-precipitates (Fig. 5), which is in agreement with previous observations that γ′ and γ″ are co-located in Inconel 718 [19,20], forming a sandwich-like structure of the form γ′/γ″/γ′ or γ″/γ′/γ″ [20] with interfaces between the γ′ and γ″ on the (0 0 1)γ″/{0 0 1}γ′ planes. The present study confirms that such co-precipitation occurs even in the earliest stages of ageing.

A direct correlation can be made between the increase in hardness observed in Fig. 1 and the precipitation observed in the TEM and atom probe data, confirming that the hardening can be directly

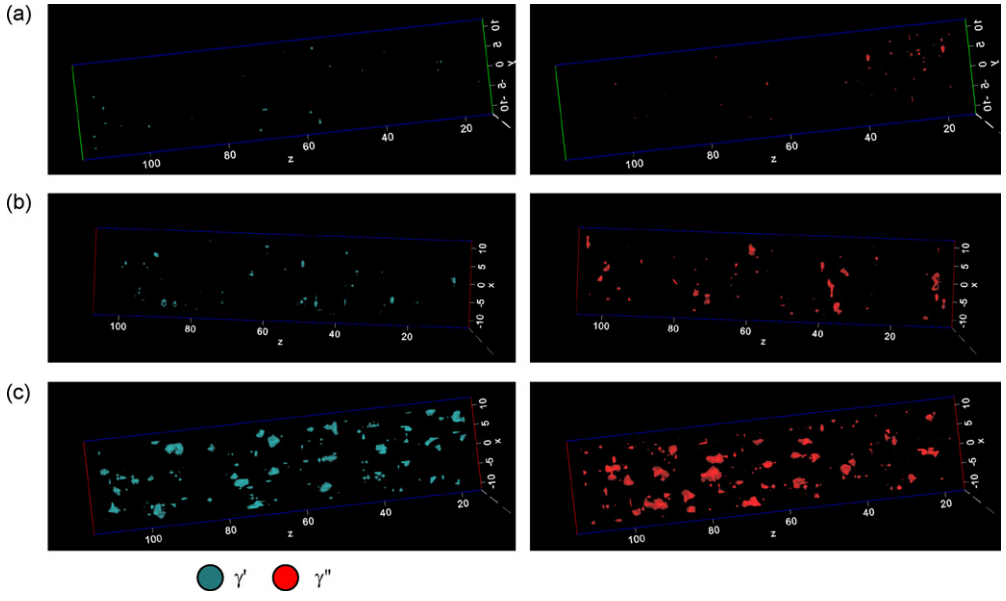

Fig. 4. Atom probe data showing Al + Ti (γ′) and Nb (γ″) isoconcentration surfaces (10 at.%) in samples aged for a) 120 s; b) 500 s; c) 5000 s.

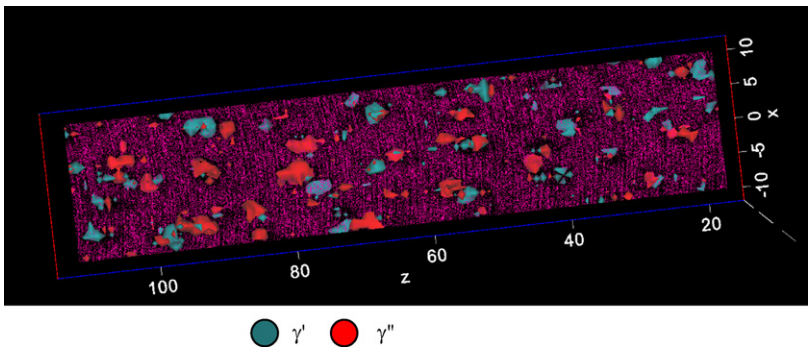

Fig. 5. Co-precipitation of γ′ and γ″ observed in the sample aged 5000 s. Each pink dot is an atom of Cr or Fe and isoconcentration surfaces of 10 at.% Al + Ti or Nb were used to reveal the location of the precipitates. (For interpretation of the references to colour in this figure legend, the reader is referred to the web version of the article.)

attributed to the precipitation of γ′ and γ″ phases. For these small precipitates, the hardening is expected to be the result of coherency strains between the precipitates and the matrix [21] and order strengthening (dislocations cutting the particles will create an anti-phase boundary unless they are travelling in pairs) [7,18].

The volume fraction of each of the precipitates observed after ageing for 500 s and 5000 s was approximated from the atom probe data by measuring the volume inside the 10% isoconcentration surfaces used to generate the images shown in Fig. 4. This data is plotted in Fig. 6. The volume fraction of the γ″ was calculated to be higher than that of γ′ and, while they both increased with ageing, the ratio of γ″/γ′ was higher for the sample aged for 500 s (i.e. there was a higher proportion of γ″ in the earlier stage of ageing).

To improve creep properties trace amounts of boron and phosphorus are added to WE-91 in the ppm range [1–3,5]. However, these trace elements have detrimental effects on the weldability of this alloy. APT also was used to compare the concentration of these elements in the precipitate and matrix regions, but no significant difference in the boron or phosphorous concentration was observed between the matrix and the precipitates.

For specimens in which precipitation could not yet be observed (the AQ specimen and the specimen aged for 120 s), the dataset was analysed to determine whether any pre-precipitation 'clustering' was present. The 'Core Linkage' algorithm [16] was applied to the datasets to search for 'clusters' (groups of atoms of particular species that are clustered together for thermodynamically favourable reasons). It provides information about the clustering detected in the dataset, and compares this to the amount of clustering that would be expected if the atoms were randomly distributed. The algorithm requires the selection of three parameters, namely d_{max}, d_{link} and N_{min}. Details of the significance of these parameters are provided elsewhere [16]. The minimum number of atoms for a cluster (N_{min}) was chosen to be 5, as larger clusters are expected to better represent the earliest signs of precipitation. Optimised values of d_{max} and d_{link} were selected that provided the clearest indication of the deviation from random. In order for the results to be comparable a volume of 30 nm × 30 nm × 40 nm was selected from each of the original AP datasets for analysis.

In order to compare the extent of clustering, the proportion of solute atoms found to be contained in a cluster is shown in Fig. 7 for the AQ and 120 s aged samples, where Ti/Al clustering is thought to be a precursor to precipitation of γ′ and Nb clustering is thought to lead to γ″ formation. Fig. 8 shows the number of clusters in the selected volume as a function of cluster size (i.e. the number of atoms in the cluster) for Ti/Al and Nb.

A significant increase in the proportion of Nb forming clusters (Fig. 7) is observed after 120 s of ageing, while there is a much smaller increase in the proportion of Ti/Al atoms in clusters after the same ageing period. The histogram (Fig. 8) shows that the increase in Nb clustering is across the entire size range. It is possible that the slight increase in hardness already observed in the specimen aged for 120 s could be attributed to the pre-precipitate clustering of Nb prior to precipitation of γ″. This clustering may also suggest that, although both γ′ and γ″ are present as co-precipitates very early in the ageing process, γ″ forms first. This is also consistent with the observation in the atom probe data that the proportion of the γ″ (as a fraction of the overall volume of precipitates) is higher in the earlier stages of ageing.

Cozar and Pineau [22] found that superalloys with a ratio of the combined Al + Ti at.% to Nb at.% of > 0.8 favour the formation of γ′ prior to γ″ precipitation and that if the ratio is < 0.8 no precedence of one precipitate over another is observed [9,10] (the samples studied here have a Al + Ti/Nb ratio of ~0.7). Sundararaman et al. [23] investigated precipitation by TEM in an alloy where this ratio was 0.66.

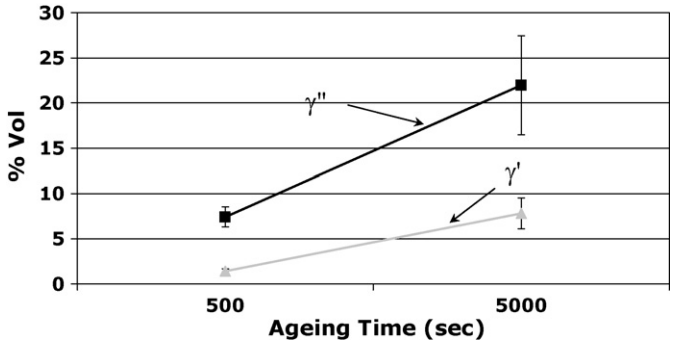

Fig. 6. Volume fraction of γ′ and γ″ measured for specimens aged for 500 s and 5000 s. The error bars are estimated based on the changes in the measured values depending on (i) the isoconcentration surface value used to define the edge of the precipitate and (ii) the voxel size selected in the data reconstruction software. The line between the points is included as a guide to the eye only.

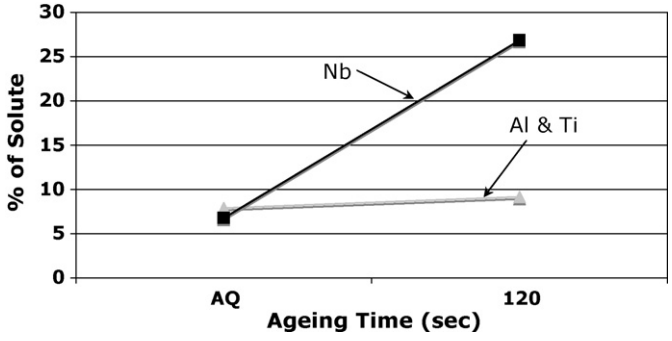

Fig. 7. Plot of the percentage of solute atoms that are clustered in the as-quenched sample and the sample aged for 120 s. The line between the points is included as a guide to the eye only.

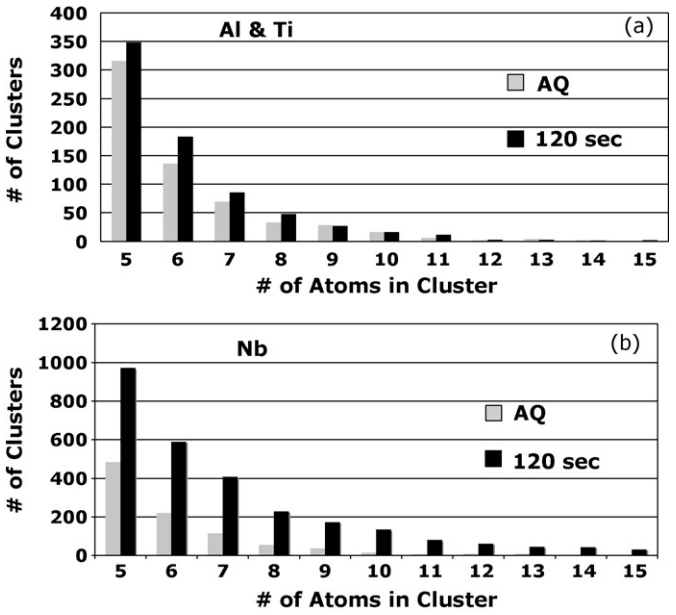

Fig. 8. A cluster size histogram for the as-quenched and 120 s aged conditions. a) Al and Ti and b) Nb.

Although they were able to demonstrate that γ' does not precede γ'' in their alloy, they point out that, due to the difficulty distinguishing γ' in the TEM where γ'' is present, it was not possible to ascertain whether the precipitation of both phases occurs in a simultaneous manner or whether γ'' particles appear first. However, in previous atom probe investigations of precipitation in Inconel 718, Miller [11] showed evidence that, at the initial stage of precipitation their 'secondary' γ'' precipitates were Nb-enriched, indicating that the initial nucleus is the γ'' phase in an alloy with a Al + Ti/Nb ratio of ~0.66. Miller's results are in good agreement with our present observations of increased Nb clustering immediately prior to precipitation and the relatively high volume fraction of γ'' seen at the earliest stage at which precipitates were observed (500 s).

4. Conclusions

TEM and atom probe confirmed that hardening in the early stages of ageing in IN718 can be directly attributed to the precipitation of γ' and γ'' phases. Precipitation was first observed after 500 s of ageing at 706 °C. The γ' and γ'' precipitates were often co-located. While the volume fraction of γ'' was greater at all stages of ageing, the ratio of γ''/γ' was higher in the earlier stages.

Analysis of atom probe datasets from samples aged for shorter periods, in which precipitates were not observed, showed a non-random distribution of the Al, Ti and Nb, indicating the presence of clustering prior to precipitation. While the extent of Al/Ti and Nb clustering was quite similar in the as-quenched sample, the extent of Nb clustering increased significantly in the sample that had been aged for 120 s, while the Al/Ti clustering increased only slightly.

It is therefore thought that, although both γ' and γ'' precipitates are both present from the earliest stages of ageing at which the precipitates could be observed, the γ'' precipitation precedes the γ' precipitation during ageing in this alloy.

Acknowledgements

Funding for this work from Australian Research Council is gratefully acknowledged. The authors are also grateful for scientific and technical input and support from the Australian Microscopy & Microanalysis Research Facility (AMMRF) node at The University of Sydney, particularly Mr. Alex La Fontaine and Mr. Adam Sikorski for their advice and suggestions on sample preparation, Leigh Stephenson and Sha Li for advice on clustering analysis and Dr. Ting-Yu Wang for help with the TEM work. The authors would like to thank Allvac and Dr. Wei-D Cao for providing the alloy.

References

[1] S. Benhadad, N.L. Richards, M.C. Chaturvedi, Metall. Mater. Trans. A 33 (2002) 2005–2017.
[2] B.C. Yan, J. Zhang, L.H. Lou, Mater. Sci. Eng., A 474 (2008) 39–47.
[3] C.G. McKamey, C.A. Carmichael, W.D. Cao, R.L. Kennedy, Scripta Mater. 38 (1998) 485–491.
[4] E. Cadel, D. Lemarchand, S. Chambreland, D. Blavette, Acta Mater. 50 (2002) 957–966.
[5] L. Xiao, D. Chen, M.C. Chaturvedi, J. Mater. Eng. Perform. 14 (2005) 528–538.
[6] D. Blavette, E. Cadel, C. Pareige, B. Deconihout, P. Caron, Microsc. Microanal. 13 (2007) 464–483.
[7] C. Sims, N. Stoloff, W. Hagel, Superalloys II, John Wiley & Sons, 1987.
[8] C. Slama, M. Abdellaoui, J. Alloys Compd. 306 (2000) 277–284.
[9] C. Slama, C. Servant, G. Cizeron, J. Mater. Res. 12 (1997) 2298–2316.
[10] K. Nakai, Y. Ohara, H. Ohtsubo, Y. Ohmori, ISIJ Int. 36 (1996) 187–193.
[11] M.K. Miller, Micron 32 (2001) 757–764.
[12] M.G. Burke, M.K. Miller, Colloque De Physique 50 (1989) 395–400.
[13] M.G. Burke, M.K. Miller, in: A. Edward, Loria (Eds.), The Minerals, Metals & Materials Society, 1991, pp. 337–350.
[14] M.K. Miller, Atom Probe Tomography: Analysis at the Atomic Level, 1st ed., Kluwer Academic/Plenum Publishers, New York, 2000.
[15] D.H. Ping, Y.F. Gu, C.Y. Cui, H. Harada, Mater. Sci. Eng., A 456 (2007) 99–102.
[16] L.T. Stephenson, M.P. Moody, P.V. Liddicoat, S.P. Ringer, Microsc. Microanal. 13 (2007) 448–463.
[17] D.F. Paulonis, J.M. Oblak, D.S. Duvall, Trans. ASM 62 (1969) 611–622.
[18] R.C. Reed, The Superalloys: Fundamentals and Applications, 1st ed., Cambridge University Press, Cambridge, 2006.
[19] M.K. Miller, S.S. Babu, M.G. Burke, Mater. Sci. Eng., A 270 (1999) 14–18.
[20] W.T. Geng, D.H. Ping, Y.F. Gu, C.Y. Cui, H. Harada, Phys. Rev. B: Condens. Matter Mater. Phys. 76 (2007), 224102 (1–10).
[21] M.C. Chaturvedi, Y.F. Han, Met. Sci. 17 (1983) 145–149.
[22] R. Cozar, A. Pineau, Metall. Trans. 4 (1973) 47–59.
[23] M. Sundararaman, P. Mukhopadhyay, S. Banerjee, Metall. Mater. Trans. A 23 (1992) 2015–2028.